Geol. Mag. **147** (*1*), *2010, pp. 59–76. © Cambridge University Press 2009*
doi:10.1017/S0016756809990021

Skeletal carbonate productivity and phosphogenesis at the lower–middle Cambrian transition of Scania, southern Sweden

J. JAVIER ÁLVARO*†, PER AHLBERG‡ & NIKLAS AXHEIMER‡

*Departamento Ciencias de la Tierra, Universidad de Zaragoza, E-50009 Zaragoza, Spain
‡GeoBiosphere Science Centre, Department of Geology, Lund University, Sölvegatan 12, SE-223 62 Lund, Sweden

(*Received* 12 March 2008; *accepted* 16 February 2009; First published online 16 June 2009)

Abstract – The lower–middle Cambrian transitional interval of Scania is largely represented by condensed limestone beds, lithostratigraphically grouped in the Gislöv Formation (1–5.7 m thick), and the Forsemölla and Exsulans Limestone beds (lower part of the Alum Shale Formation, up to 4 m thick). The strata display a combination of skeletal carbonate productivity, episodic nucleation of phosphate hardground nodules, and polyphase reworking recorded on a platform bordering the NW corner of Baltica. The shell accumulations can be subdivided into three deepening-upward parasequences, separated by distinct erosive unconformities. The parasequences correspond biostratigraphically to the *Holmia kjerulfi*, *Ornamentaspis*? *linnarssoni* and *Ptychagnostus gibbus* zones, the latter two generally being separated by a stratigraphic gap that includes the middle Cambrian *Acadoparadoxides oelandicus* Superzone. Except for the Exsulans Limestone, the carbonates reflect development of a prolific epibenthic biota, dominated by filter-feeding nonreefal chancelloriid–echinoderm–sponge meadows, rich in trilobites and brachiopods, and which were subjected to high-energy conditions. The absence of microbial mats or veneers encrusting the erosive surfaces of these event-concentration low-relief shoal complexes may be related to long hiatal episodes resulting in microboring proliferation. High levels of nutrient supply resulted in high primary productivity, eutrophic conditions, glauconite precipitation, phosphogenesis (in some case microbially mediated) and microendolithic infestation. An early-diagenetic mildly reducing environment is suggested by the presence of authigenic (subsequently reworked) pyrite, which contrasts with the syndepositional normal oxygenated conditions reflected by macroburrowing and the abundance of benthic fossils.

Keywords: carbonate productivity, apatite, glauconite, chemostratigraphy, Baltica.

1. Introduction

The early–middle Cambrian transitional interval was a time of significant environmental and global biotic changes, due to the interplay of: (1) a worldwide transition from regressive to transgressive conditions punctuated by diachronous erosive unconformities (e.g. Palmer & James, 1980; Álvaro & Vennin, 1998; Nielsen & Schovsbo, 2007; references therein), (2) a distinct replacement of benthic communities, regionally related to extinction events and the virtual disappearance of archaeocyathan–microbial frame-building fabrics (Debrenne, 1991; Álvaro *et al*. 2003) and (3) a sharp modification of biogeographic interconnections in peri-Gondwanan, Siberian and Baltic margins, leading to a significant increase in cosmopolitan trilobite assemblages and the establishment of the middle Cambrian Acado-Baltic Province (*sensu* Sdzuy, 1972). The global correlation of the traditional lower–middle Cambrian (or provisional Cambrian Series 2–3: Babcock *et al*. 2005) boundary interval is a matter of debate, due to the presence of numerous erosive unconformities, condensation levels, the endemic character of most biostratigraphically significant taxa, and the lack of high-resolution stratigraphic studies (for a discussion of West Gondwana, see Álvaro & Clausen, 2005). As a result, integrated chemo-, event- and sequence-stratigraphic analyses are necessary to identify problems related to stratigraphic completeness and time resolution of this Series transition, two key factors for palaeogeographic reconstructions and chemostratigraphic correlation.

According to palaeomagnetic data (Torsvik & Rehnström, 2001), Baltica was geographically inverted and lay at temperate–subtropical palaeolatitudes (~ 30–60° S) during Cambrian times. The early–middle Cambrian transition is represented by several episodes of carbonate productivity in Scania (southern Scandinavia) and along the Caledonian Front in southern Norway and NW Sweden (e.g. the Sjoutälven, Högnäsån and Sörsjön areas of the Tåsjön detachment in northern Jämtland and southern Västerbotten, and the Laisvall–Storuman and Torneträsk areas in Lapland; see, e.g. Gee, Kumpulainen & Thelander, 1978; Ahlberg, 1983; Greiling, Jensen & Smith, 1999; Moczydłowska *et al*. 2001; Axheimer, Ahlberg & Cederström, 2007). Previous works have noted the incompleteness of these thin, carbonate-dominated successions due to the distinctiveness of their intra-bed erosive unconformities (for a synthesis, see Nielsen & Schovsbo, 2007). In Baltica, the traditional base of the 'Middle Cambrian' (or 3rd Cambrian Series) *sensu*

†Author for correspondence: jjalvaro@unizar.es

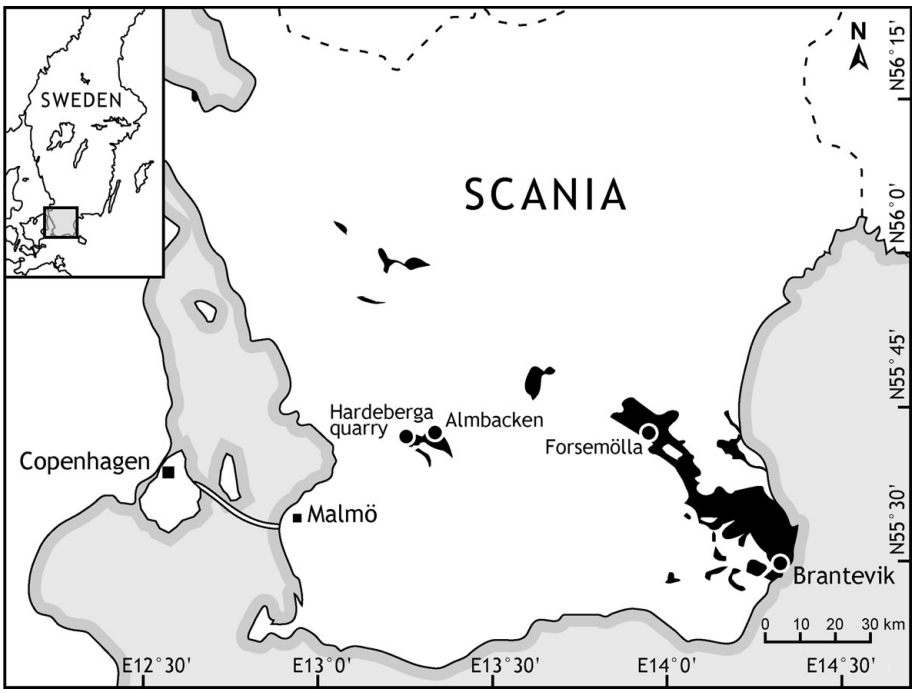

Figure 1. Map of Scania, southern Sweden, showing major Cambrian outcrop areas (black) and the location of Brantevik, Forsemölla, Hardeberga, and the Almbacken borehole; modified from Martinsson (1974, fig. 7).

Brøgger (1886) has generally been placed at the first appearance of *Paradoxides s.l.*

The aim of this paper is to analyse the high-resolution stratigraphic patterns of the unconformity-bearing mixed (carbonate–siliciclastic) strata that include the traditional lower–middle Cambrian boundary interval in Scania (Skåne), southern Sweden (NW corner of Baltica).

2. Geological setting and stratigraphy

In Scania (Fig. 1), the lower–middle Cambrian boundary interval displays a broad transition from regressive to transgressive conditions. These are represented by a stratigraphic evolution from proximal coarse-grained siliciclastic strata to distal kerogen-rich shales, which are punctuated by discrete carbonate beds. In ascending order, the transitional interval is represented by the Rispebjerg Member (upper Læså Formation), the Gislöv Formation and the lowermost part of the Alum Shale Formation, including the Forsemölla and Exsulans Limestone beds (for a recent lithostratigraphic revision, see Nielsen & Schovsbo, 2007; Fig. 2). The Rispebjerg Member is a thin, 1–3 m, homogeneous succession of calcareous medium- to coarse-grained quartz sandstone, with phosphorite clasts mainly restricted to the basal conglomerates, and impregnation of authigenic phosphorite in its uppermost part (de Marino, 1980*a*; Bergström & Gee, 1985; Pedersen, 1989). Except for some fragmentary shelly fossils, the only fossils observed in Scania are ichnofossils near the top of the formation (Lindström & Staude, 1971; Bergström & Ahlberg, 1981). The Rispebjerg Member is unconformably overlain by the Gislöv Formation, a thin (0.7–5.7 m) heterolithic unit that consists of fossiliferous silty limestone, siltstone and claystone. It is rich in glauconite and phosphatic clasts (de Marino, 1980*b*), and has yielded trilobites indicative of the *Holmia kjerulfi* and *Ornamentaspis*? *linnarssoni* assemblage zones (late early Cambrian: Bergström & Ahlberg, 1981). The contact between the Gislöv and the Alum Shale formations is laterally variable: at Forsemölla (Figs 1, 2), the contact is situated at the base of a medium grey to black shale (the so-called *ritskiffer* or 'drawing shale'; middle Cambrian according to Nielsen & Schovsbo, 2007), which is about 50 cm thick and has yielded a few linguliformean brachiopods and hyoliths (Bergström & Ahlberg, 1981). In other outcrops, the contact is a simple discontinuity surface underlying the Forsemölla Limestone Bed (Nielsen & Schovsbo, 2007). This limestone unit has yielded paradoxidid remains belonging to *Hydrocephalus* sp. (Forsemölla section) and *Paradoxides paradoxissimus* (Brantevik section: Bergström & Ahlberg, 1981), suggesting the presence of a stratigraphic gap that is broadly equivalent to the *Acadoparadoxides oelandicus* Superzone (Fig. 2).

The middle Cambrian part of the Alum Shale Formation has a thickness of 20–40 m and consists of dark grey to black, kerogen- and sulphide-rich shale with lenses or beds of dark grey limestone. They accumulated over long periods of time, changing from middle Cambrian oxygenated to Furongian dominantly dysoxic, anoxic or euxinic conditions (A. T. Nielsen, Copenhagen, pers. comm. 2009). Four distinctive and correlatable, middle Cambrian limestone beds, all less than 1 m thick, are interbedded within this monotonous clayey succession: the Forsemölla (formerly referred

https://doi.org/10.1017/S0016756809990021 Published online by Cambridge University Press

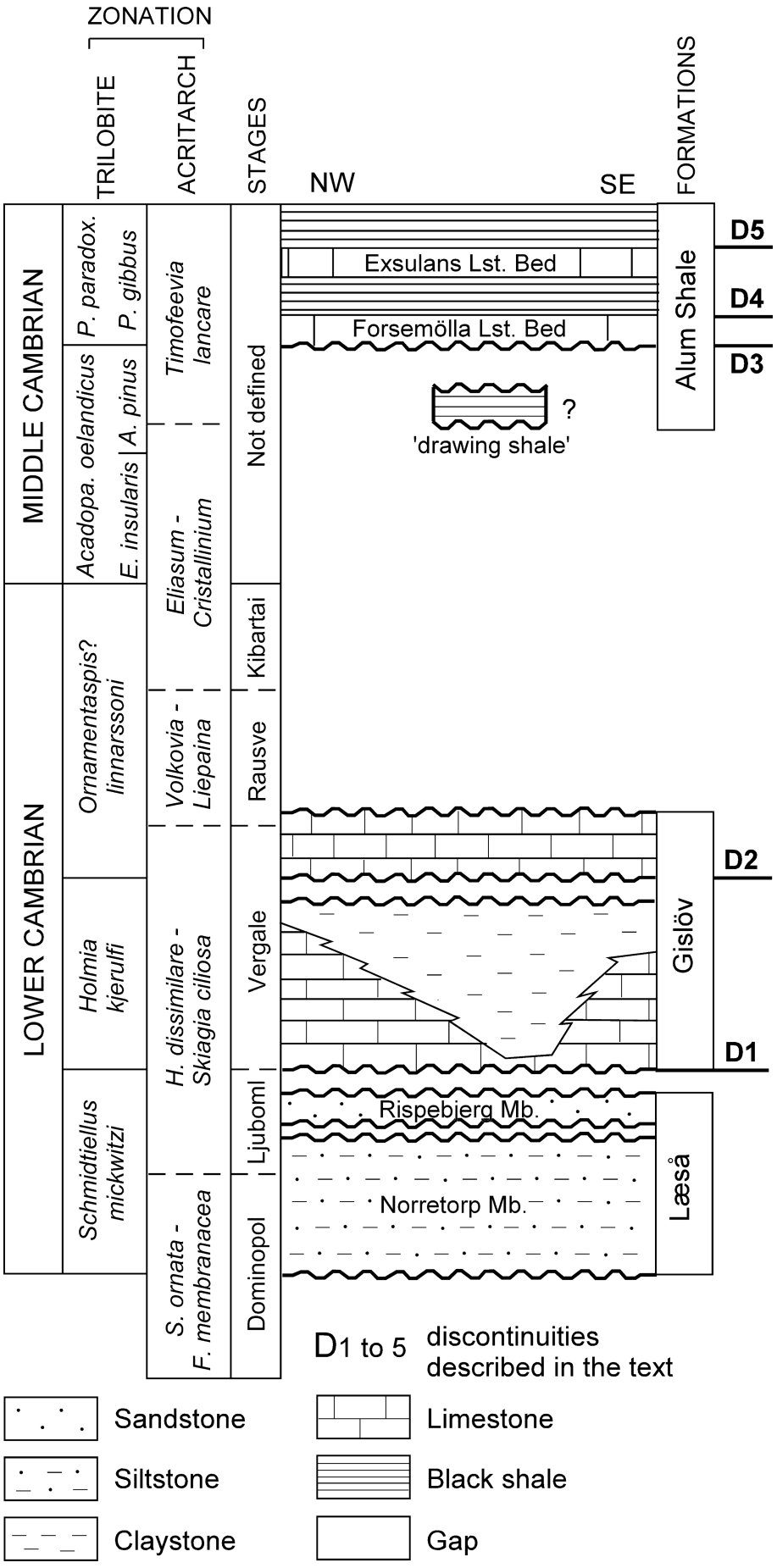

Figure 2. Stratigraphic units of the lower–middle Cambrian transition in Scania; modified from Nielsen & Schovsbo (2007).

https://doi.org/10.1017/S0016756809990021 Published online by Cambridge University Press

to as 'fragment'), Exsulans, Hyolithes and Andrarum Limestone beds (Ahlberg, 1998; Ahlberg & Bergström, 1998; Axheimer & Ahlberg, 2003; Nielsen & Schovsbo, 2007).

From a biostratigraphic point of view, sediments attributed to the *Holmia kjerulfi* Assemblage Zone and correlative strata in Poland (*Holmia* Zone) display an association of olenellid and ellipsocephalid trilobites, the former dominated by *Holmia* and *Kjerulfia*, and the latter by *Ellipsocephalus*, *Proampyx*?, *Ornamentaspis*? and *Strenuaeva*. The presence of eodiscoids (*Calodiscus lobatus* and *Runcinodiscus* cf. *index*) in the *Holmia kjerulfi* Assemblage Zone suggests a correlation with strata containing representatives of the *Serrodiscus bellimarginatus–Triangulaspis annio–Hebediscus attleborensis* assemblage (Robison *et al*. 1977; Ahlberg, 1983; Geyer, 2005) in the North Atlantic region and Siberia, for example, with the '*Callavia*' Zone in Avalonia and the middle Botoman substage in Siberia.

The latest early Cambrian zone in Scandinavia, the *Ornamentaspis*? *linnarssoni* Assemblage Zone (previously referred to as the *Strenuella linnarssoni* Zone), was established by Kiær (1917) for a succession of shales and a few interbedded limestones (the Evjevik Limestone) that overlie the Holmia Shale (Tømten Member of Nielsen & Schovsbo, 2007) in the Mjøsa area, southern Norway. This zone has been recorded with certainty only in southern Norway and Scania. In Scania, the base of the zone is placed at the first appearance of *O*.? cf. *linnarssoni* (Kiær, 1917) within the middle part of the Gislöv Formation (Bergström & Ahlberg, 1981). The trilobites of the zone are dominated by ellipsocephalids, but also include rare specimens of olenellids (*Holmia kjerulfi* and *Kjerulfia lata*: Ahlberg & Bergström, 1978; Nikolaisen, 1986). The zone may be tentatively correlated with the lower part of the *Protolenus* Zone in Poland (Moczydłowska, 1991).

A few pygidia of paradoxidid trilobites have been recovered from the Forsemölla Limestone Bed, which seems to represent the lowermost part of the middle Cambrian *Paradoxides paradoxissimus* Superzone (Bergström & Ahlberg, 1981). This limestone unit has also yielded fairly rich faunal assemblages, including trilobites, linguliformean brachiopods, echinoderm ossicles, hyolithids, helcionellids, lapworthellids, hyolithelminthids, bradoriids, palaeoscolecids, phosphatocopids and conodont-like elements (Bengtson, 1976; de Marino, 1980*b*; Streng, Geyer & Budd, 2006; Streng *et al.* 2007). The middle Cambrian *Acadoparadoxides oelandicus* Superzone is generally absent in Scania and corresponds to a hiatus between the Gislöv Formation and the Forsemölla Limestone Bed. Locally, however, a succession of dark grey to black shales is present between the top of the Gislöv Formation and the base of the Forsemölla Bed, for instance, in the Almbacken drill core (Axheimer & Ahlberg, 2003). This shale unit was assigned to the *A. oelandicus* Superzone by Nielsen & Schovsbo (2007).

3. Facies associations

Three sections and one drill core have been studied in order to characterize the facies associations of the Gislöv Formation and the Forsemölla and Exsulans Limestone beds: (1) the stratotype of the Gislöv Formation, about 1 km SW of Brantevik in eastern Scania, (2) the Forsemölla section in eastern Scania, (3) a section through the upper lower Cambrian at the Hardeberga quarry in south-central Scania (Bergström & Ahlberg, 1981) and (4) a drill core from Almbacken, east of Lund in south-central Scania (Axheimer & Ahlberg, 2003) (Fig. 1). The lithological succession and the facies associations in the outcrops were briefly described by de Marino (1980*a*, *b*) and Bergström & Ahlberg (1981), who also provided references to earlier studies dealing with the lower–middle Cambrian transition in Scania. Graphic logs and correlation lines are shown in Figure 3.

3.a. Bioclastic limestone bearing millimetre-scale skeletons (Gislöv Formation)

The limestone consists of well-bedded to partly nodular wackestone to packstone, usually thin-bedded and slightly to moderately burrowed (Fig. 4a, b). Centimetre-thick fining-upward units, resting on scoured surfaces, are common (Fig. 4c). Intra-bed irregular surfaces are commonly lined with anastomosing swarms of clay seams, up to 1 cm thick. Trilobites and calcitic brachiopods are abundant, whereas echinoderm ossicles, linguliformean brachiopods, chancelloriid sclerites, sponge spicules, bradoriids (Dies Álvarez *et al*. 2008) and other skeletonized microfossils of uncertain affinity are subsidiary. The fossils are predominantly fragmented and abraded, and commonly display a chaotic (random orientation) fabric, although they are locally imbricated or arranged in crude low-angle laminae. The content of silt- to fine-grained sand-sized siliciclastic material is highly variable, and rare glauconitic and phosphatic clasts are encountered in thin-section.

The local abundance of fenestral-like cavities may impart a mottled aspect to the Gislöv Formation. Primary pore types include intra- and interparticulate shelter pores, up to 3 mm in size. The latter are lined with early isopachous fibrous calcite crystals, up to 30 μm in length, and later by mosaics of inclusion-rich calcite cements. Equant sparry calcite cements (anhedral to subhedral crystals, 50–100 μm in size) occur geopetally in mouldic pores, and syntaxial cements commonly surround the echinoderm ossicles. Spar-filled fenestral-like vugs, cutting both matrix and skeletons, are common in some strata (Fig. 4d).

The presence of low-angle lamination and millimetre-scale fragmented bioclasts, arranged in graded units and underlain by erosive contacts, suggests that the substrate was winnowed, probably by the action of waves and storm episodes. The patchy abundance of bioturbation associated with infaunal deposit feeders

https://doi.org/10.1017/S0016756809990021 Published online by Cambridge University Press

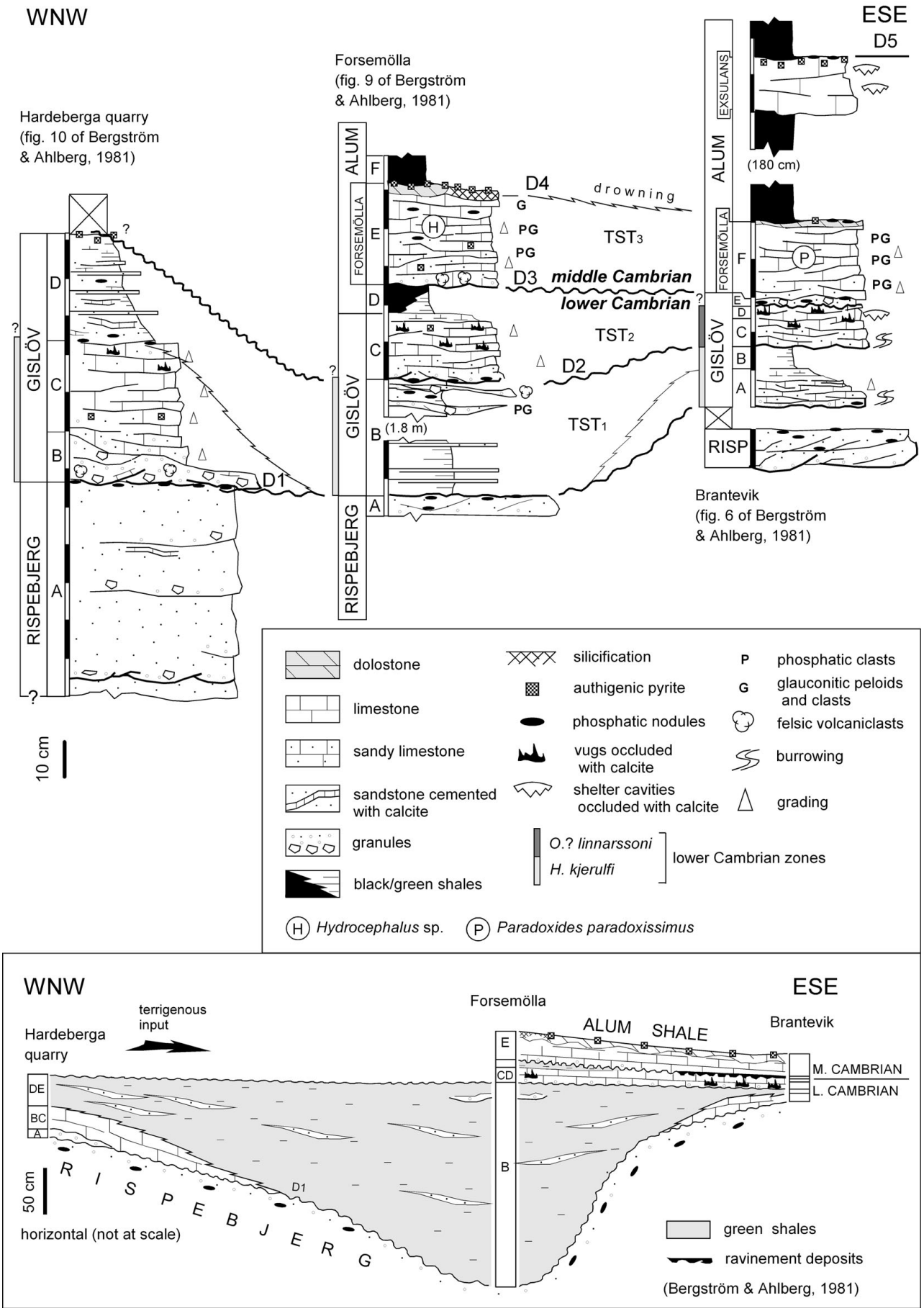

Figure 3. Stratigraphic logs of the study areas, with reference to Bergström & Ahlberg's (1981) nomenclature, and reconstruction of the sedimentary architecture of the Gislöv and Forsemölla units.

https://doi.org/10.1017/S0016756809990021 Published online by Cambridge University Press

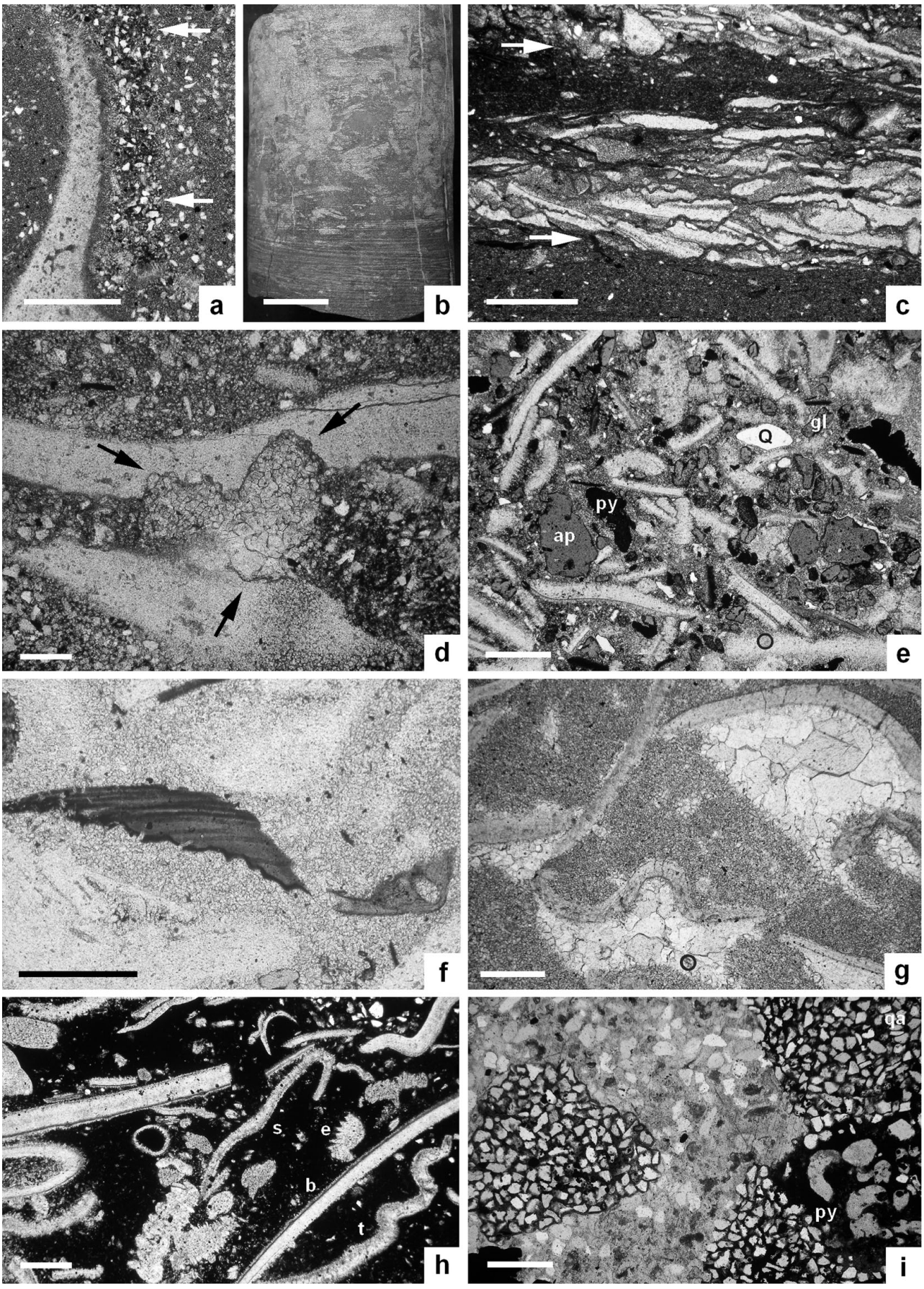

Figure 4. For legend see facing page.

https://doi.org/10.1017/S0016756809990021 Published online by Cambridge University Press

indicates that benthic colonization of the sea-floor was not inhibited by synsedimentary or early diagenetic cementation. The diversity of the shelly fauna suggests that deposition took place in an open-sea environment of normal salinity. Partial dissolution is suggested by the presence of a secondary vuggy porosity, recognizable by the embayed morphology of the pores and their cross-cutting of pre-existing bioclastic fabrics. This reflects circulation of undersaturated waters. As the vuggy cavities were apparently not connected with the surface, precluding a karstic origin, they must be associated with other solution processes. Finally, anastomosing swarms of clay seams represent late-diagenetic dissolution of carbonate and relative enrichment of clay displaying solution-seam fabrics.

3.b. Glauconite–phosphate calcarenite (Forsemölla Limestone Bed)

The calcarenite, less than 1 m thick, displays clay and carbonate mud contents ranging from 50 to 70 % in volume. The remaining framework consists of a heterogeneous packstone, with evenly disseminated silt- to medium-grained sand-sized clasts, millimetre- to centimetre-sized phosphate clasts and nodules and glauconitic peloids and clasts (Fig. 4e). Low-angle laminae and intra-bed irregular surfaces, overlain by millimetre- to centimetre-scale (normal) graded laminae, are common. Lithic extraclasts consist of mono- and polycrystalline quartz, feldspar, mica flakes, opaques and rip-up shale clasts. Bioclasts are dominated by linguliformean brachiopods (Fig. 4f), trilobites, bradoriids and echinoderm ossicles. The skeletons occur both as isolated debris and embedded within composite clasts. The latter contain first-generation skeletons, accretionary sediment and calcite and phosphate cements truncated at borders. Pyrite consists of single and composite grains dispersed throughout the microsparry calcite. All the aforementioned components can be coated with single or multiple layers of collophane. The top of the bed is partly dolomitized and rich in authigenic phosphate and pyrite.

As noted in the previous facies association, the sedimentary structures indicate winnowing, probably developed by the action of waves and episodic storms. However, both the fossil assemblage and the allochems (here dominated by phosphate and glauconite clasts) are different. The presence of multiphase clasts indicates that at least parts of the sea-floor were lithified when reworked. Reworking of pyrite is also shown by mechanical breakage of pyrite grains and the polyphase nature of some compound pyrite agglomerates.

3.c. Bioclastic limestone bearing centimetre-scale skeletons (Exsulans Limestone Bed)

The Exsulans Limestone Bed, up to 60 cm thick, is composed of bioclastic mudstone to packstone. Larger bioclasts average about 2 cm in size, and reach sizes of 6 cm in outcrop. The skeletal elements consist of trilobites (up to 80 % in volume), and subsidiary calcite-walled brachiopods and echinoderm ossicles, along with hyoliths and taxa of uncertain affinity. The skeletons are both disarticulated and to some extent articulated. Partial geopetal infills of internal cavities (commonly articulated brachiopods) and abundant shelter infills (with sparry occlusions similar to those described in Section 3.b; Fig. 4g) are parallel to the stratification plane. The top of the bed is partly dolomitized and rich in authigenic phosphate and pyrite (Fig. 4h).

The high mud content, preservation of a non-fragmentary fauna, and the lack of scouring features and internal lamination suggest that deposition occurred in a low-energy, deep and oxygenated subtidal environment. There is no evidence of discontinuous reworking, and abrasion and fragmentation of skeletons is minimal. The end of this palaeoenvironment is related to extensive flooding and the subsequent (and post-depositional) precipitation of authigenic minerals under suboxic conditions.

3.d. Homogeneous to bedded shale (Gislöv Formation)

The shale consists of irregularly bioturbated, dark grey to brownish claystone interbedded with thin-bedded siltstone. The carbonate content commonly changes

Figure 4. Thin-section photomicrographs of the Gislöv Formation, and the Forsemölla and Exsulans Limestone beds. (a) Millimetre-scale burrow (arrowed) partly infilled with silt-grained quartz and a darker mixture of calcite and iron oxides; Bergström & Ahlberg's (1981, fig. 6) level A at Brantevik; scale bar = 1 mm. (b) Portion of the Almbacken drill core (depth: 31.80 m) showing the mottled aspect of the limestones in the Gislöv Formation due to burrowing; scale bar = 2 cm. (c) Millimetre-thick, packstone-to-wackestone, grading units, underlain by erosive surfaces (arrowed), and embedded in a micritic matrix; lower part of Bergström & Ahlberg's (1981, fig. 9) level C at Forsemölla; scale bar = 1 mm. (d) Cross-cutting feature of a solution vug, occluded by a mosaic of calcite crystals, and subsequently microstylolitized; Bergström & Ahlberg's (1981, fig. 6) level C at Brantevik; scale bar = 1 mm. (e) Ravinement deposit of Bergström & Ahlberg's (1981, fig. 6) level E at Brantevik, showing a trilobite-dominated packstone and dispersed apatite (ap), glauconite (gl), pyrite (py), and quartz (Q) clasts; scale bar = 1 mm. (f) Same level exhibiting two phosphate-walled linguliformean fragments; scale bar = 0.5 mm. (g) Centimetre-long sclerites of trilobites underlain by shelter porosities occluded with mosaics of calcite crystals; base of Exsulans Limestone Bed at Brantevik; scale bar = 2 mm. (h) Packstone rich in trilobites (t), brachiopods (b), echinoderm ossicles (e) and sponge spicules (s) embedded in a pyritic cement; bioclasts covered by fibrous calcite cements; top of Exsulans Limestone from core drilling at Almbacken; scale bar = 2 mm. (i) Detail of conglomeratic lag lining a channel, containing quartz arenitic (qa), litharenitic and pyritic (py) granules embedded in a litharenite cemented by calcite; base of Bergström & Ahlberg's (1981, fig. 10) level B at Hardeberga quarry; scale bar = 2 mm.

https://doi.org/10.1017/S0016756809990021 Published online by Cambridge University Press

upward from thin-bedded siltstone layers that display centimetre-thick grading, parallel, low-angle and wave lamination. Centimetre-thick limestone nodules embedded parallel to bedding, to structureless marlstone and claystone with scattered skeletal remains are also present. Thus, the presence of sedimentary structures is associated with an abrupt increase in silt content and a corresponding decrease in the carbonate content.

The shale is locally interrupted by 8 to 20 cm thick intercalations that display undulatory to faintly scoured basal contacts, which are laterally continuous on outcrop scale and consist of basal conglomerates passing upward into fine- to very fine-grained sandstones. Conglomeratic lags, covering the lowermost 5–10 cm of some beds, consist of soft, rip-up, shale clasts, calcitic brachiopod and trilobite debris and subangular granule-sized intraclasts and polyphase clasts (recognizable by the overgrowth of pyritic authigenic cements; Fig. 4i). The beds are lenticular or wedge-shaped and are commonly capped by wave-rippled and low-angle cross-laminated sets. The carbonate matrix is variable and fills intraparticular porosities and irregular millimetre-sized pockets. Axes of symmetric scoured bases show broad E–W orientations.

The centimetre-scale fining, thin to massive bedding, and upward disappearance of intercalated sandstone beds suggest that this association was deposited in an offshore environment reflecting gradual deepening. Local intercalation of scoured conglomeratic beds implies sporadic influx of coarse-grained terrigenous material.

4. Palaeoenvironments and stratigraphic discontinuities

According to a proximal–distal facies distribution, proximal facies are considered to be at the Hardeberga quarry (WNW), whereas distal sediments should be situated at Brantevik (ESE). The pattern of deposition across the lower–middle Cambrian transition can be subdivided into four asymmetric deepening-upward trends (or parasequences), 10–100 cm thick, marked by regionally developed flooding events associated with erosive discontinuities (here named D1 to D5; Figs 2, 3).

Discontinuity D1 is located at the Rispebjerg/Gislöv contact, and marks a prominent lithological change. It is recognized as an erosive surface that marks a sharp change from a siliciclastic platform, represented by the amalgamated channels and shoals of the Rispebjerg Member (de Marino, 1980*a*; Bergström & Gee, 1985; Pedersen, 1989), to a mixed (carbonate–siliciclastic) platform covered by shell pavements that gradually deepened (TST_1), grading into distal shales.

Discontinuity D2 subdivides the Gislöv Formation in two parts. It appears in outcrop as a rectilinear erosive surface that includes local undulating relief of up to 15 cm and occasional steep, centimetre-scale downward-cutting steps. Both basal lags and erosive tool marks are observed. D2 covers limestones in proximal outcrops and shales in distal ones. The succeeding deepening-upward parasequence (TST_2) consists of different facies in a proximal–distal transect; proximal outcrops (Hardeberga and Almbacken) show a siliciclastic-dominated unit, which grades from a sandstone, bearing calcite cement in patches and layers, that wedges out eastward disappearing in less than 50 km, to a silty limestone that locally passes into deeper shales.

Discontinuity D3 is a conspicuously smooth erosive unconformity with an undulating topography. It separates the Gislöv and Forsemölla units and marks the appearance of conspicuous linguliformean brachiopods (see Streng *et al*. 2007), and glauconite and phosphate peloids and clasts. The surface is associated with a substantial hiatus where the entire *Acadoparadoxides oelandicus* Superzone is generally missing. Based on these features, the formation of D3 is attributed to a sharp relative sea-level fall (although subaerial exposure features are absent) and erosion, followed by transgressive abrasion of an early-cemented shell substrate. The overlying 'E level' (*sensu* Bergström & Ahlberg, 1981, fig. 6; Fig. 3 herein), up to 2 cm thick at Brantevik and underlain by an erosive ravinement surface, is composed of polyphase intraclastic elements, abundant glauconite and phosphate clasts. The onlapping level is associated with a distinct drowning surface and was overlain by TST_3 (Eriksson, 2004; Catuneau *et al.* 2009). The transgressive unit consists of another condensed shelly limestone composed of densely packed phosphatized clasts and crudely laminated skeletal packstone/wackestone embedded in a glauconitic-rich matrix.

Discontinuities D4 and D5 are major hardgrounds that display irregular surfaces with reliefs up to 10 cm, and mark the top of the Forsemölla and Exsulans Limestone beds, respectively. They are characterized by partial dolomitization, which decreases downward, accumulation of phosphatic clasts and ubiquitous pyrite–phosphate nucleation. Dolomite and pyrite clasts are incorporated into the lowermost centimetres of the overlying black shales, suggesting early diagenetic dolomitization and pyritization processes. Both hardgrounds formed during stepwise drowning, leading to the demise of carbonate production and deposition of kerogenous shales (Alum Shale), representing deeper (darker, quieter and cooler) waters.

As a result, the onset of the four episodes of carbonate productivity: (1) took place in the central part of a mixed platform, where the nucleation of carbonate factories was bracketed between proximal, shallow-marine areas dominated by terrigenous deposition and distal, deeper-water areas where the sedimentation of clays dominated; (2) represents retrogradational (transgressive) carbonate sands, which were successively transported landward, covering increasingly larger sectors of the platform; and (3) ended by the onset of either erosive (D2 and D3) or hardground (D4 and D5) discontinuities. Although the limited lateral extension of exposures precludes determination of large-scale

https://doi.org/10.1017/S0016756809990021 Published online by Cambridge University Press

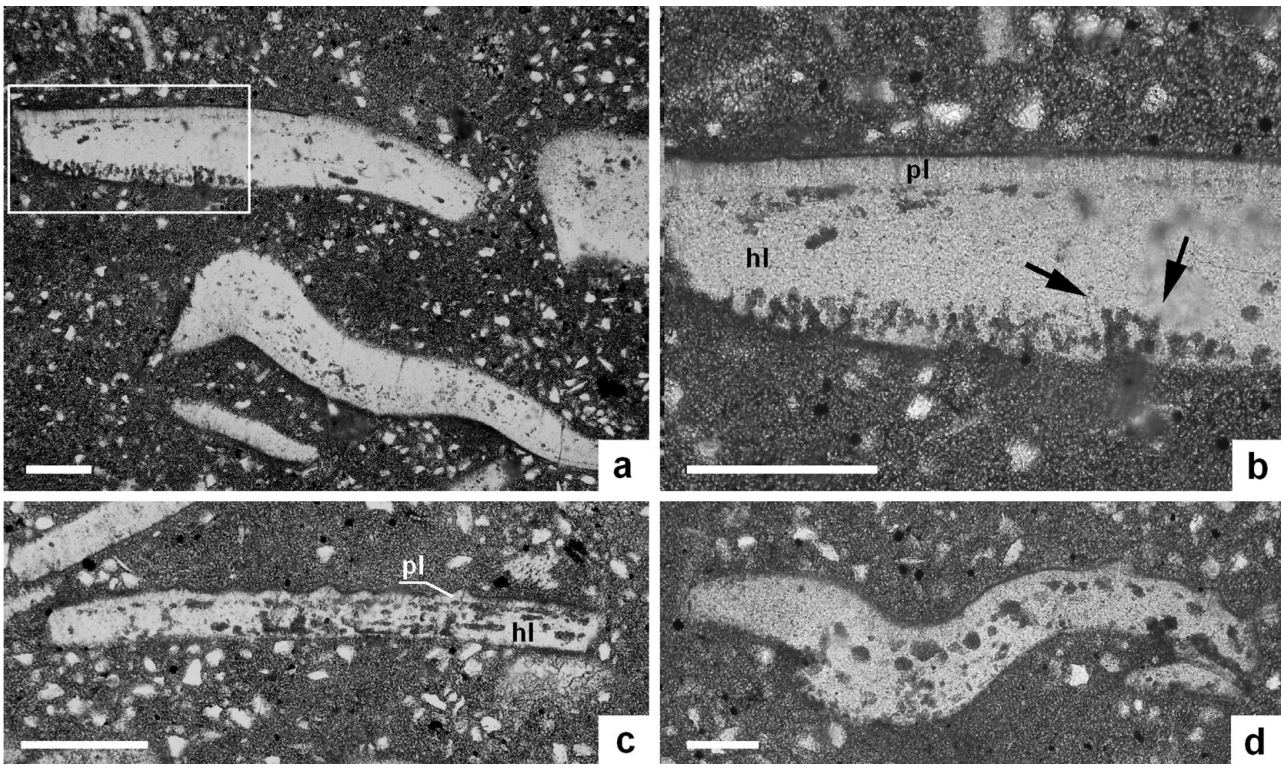

Figure 5. Thin-section photomicrographs of microboring textures from Bergström & Ahlberg's (1981, fig. 6) level E at Brantevik; all scale bars = 1 mm. (a) Mottled aspect of trilobite sclerites. (b) Detail of boxed area showing straight and Y-shaped (arrowed) microborings transverse to the skeletal wall. (c) Straight microboring parallel to skeletal wall. (d) Globular microboring, probably representing transverse sections of straight microborings. Trilobite sclerites are subdivided into a prismatic outer layer (pl) and the principal homogeneous layer (hl), the latter preferentially microbored.

sedimentary geometries, carbonate belts seemingly migrated as extensive, low-relief sheets or shoals, consisting of sediments dominated by skeletal remains that became finer with increasing distance from shoals and increasing water depth. Wave and current activity varied from just sufficient to disarticulate and transport skeletal material locally (e.g. Exsulans Limestone Bed) to sufficiently intense to accumulate beds of broken, millimetre-sized skeletal material (Forsemölla Limestone Bed). Evidence of physical abrasion in shells is mostly confined to the high-energy nearshore sediments of TST_1, TST_2 and TST_3. Relatively slow sedimentation rates for the limestones are indicated by microboring, and phosphate, pyrite and glauconite precipitation.

At the top of the Forsemölla (TST_3) and Exsulans (TST_4) units, a shift to a long-lived dysoxic–anoxic event is represented by a middle Cambrian–Furongian interval enriched in organic matter (kerogenous Alum shales), episodically punctuated by high-energy events and nucleation of carbonate productivity. The record of D4 and D5 suggests sudden and substantial deepening of the platform. As this deepening approximately coincided with a gradual sea-level rise in West Gondwana (Álvaro & Clausen, 2005), the stepwise character of the platform drowning in Scania, and the presence of complex internal and laterally rapidly changing, centimetre-thick sedimentary packages, multiple generations of intraclasts, and intra-bedded diastems of the Gislöv and Forsemölla units suggest a different subsidence regime. As noted above, these limestone beds can be traced more than 400 km north of Scania, where they maintain similar thicknesses, attesting to the flatness of the sea-floor in Baltica during Cambrian times. The kerogenous Alum shales represent the onset of a generalized drowning throughout NW Baltica. This phase of relative sea-level rise may have been important for the establishment of new biogeographic connections leading to the onset of the middle Cambrian Acado-Baltic Province (*sensu* Sdzuy, 1972) and also for the exchange of nutrient-enriched waters.

5. Microboring of shells

In thin-section, most skeletal carbonate grains of facies associations 3.1 and 3.2 show a halo of micrite affecting the outer margins as a result of complete microboring. In some cases, severe alteration has even produced entirely micritized grains. Some haloes show distinct microboring holes, occasionally in dense concentrations. These holes are either filled with carbonate micrite or microsparite, or a combination of both. Three ichnomorphotypes can be identified:

(1) Simple, cylindrical, straight to slightly curved microborings with a single, circular aperture, up to 50 μm in diameter and 300 μm long, and transverse to the skeletal wall. These are commonly unbranched microborings, although some simple branching is also observed (Fig. 5a, b).

https://doi.org/10.1017/S0016756809990021 Published online by Cambridge University Press

(2) Straight to sinuous, cylindrical microborings subparallel to the skeletal wall, displaying similar size ranges (Fig. 5c). Their ichnotaxonomic assignment is uncertain, as no complete sections connected with the surface have been observed.

(3) Scattered globular microborings, up to 200 μm in diameter, disconnected in thin-section (Fig. 5d), although their clusters are probably interconnected and represent incompletely preserved filamentous microborings of larger diameter than those described above.

The microboring organisms were host-selective. Microboring is not observed in bioclasts preserved as sparry mosaics with blocky or isopachous bladed textures, formed as a result of dissolution of unstable minerals like aragonite. Trilobite sclerites are predominantly microbored (up to 60 % of observed skeletons in some thin-sections), whereas calcitic brachiopods are rarely microbored, and echinoderm ossicles and linguliformean brachiopods show no microboring features. In addition, trilobite sclerites are not uniformly microbored. The cuticular microstructure of some trilobite sclerites consists of two layers: (1) a 'prismatic' outer layer, up to 30 μm thick with ornamentation features such as ridges and crests and (2) a principal homogeneous layer, 200 to 300 μm thick. Microboring developed predominantly in the inner homogeneous layer, reflecting its post-mortem character. Variation in microboring size appears to reflect differences in the maturity and composition of the microboring community, presumably composed of endolithic algal, fungal and/or cyanobacterial populations that rapidly infested the shell substrates. Chazotte, Le Champion-Alsumard & Peyrot-Clausade (1995) suggested that endolithic microbial infestation is very rapid in shallow water, occurring within weeks to two months.

A secondary effect of microboring was the weakening of shells, resulting in later mechanical breakage. Hence, the mixture of millimetre- and centimetre-sized bioclasts was not only controlled by hydraulic selection but also by post-mortem microboring and reworking. Since boring organisms require an onset of non-deposition intervals (Bromley & Asgaard, 1993), storm-dominated sedimentation may have controlled bioerosion, limiting the residence time of eligible hard substrates. As a result, microboring was controlled by changes in grain size, the nature of the skeletal mass bored, the rate of sediment supply, depth and frequency of storms, and the activity of infauna and epibenthos (Bromley, 2004; Glaub & Vogel, 2004; Glaub *et al.* 2007). Lower boring frequency is directly associated with enhanced siliciclastic influx, which would have increased the burial rate of host substrates and reduced their exposure time in the taphonomically active zone. On the contrary, a high density of microboring was regulated by residence time of shelly hard substrates.

6. Precipitation of fluorapatite, glauconite and pyrite

As shown in Figure 3, glauconite and fluorapatite clasts are more abundant in strata overlying the ravinement surface, at the base of the Forsemölla Limestone Bed, and in scattered conglomeratic levels. Three kinds of phosphate debris can be distinguished in the studied units:

(1) Silt- to sand-sized homogeneous clasts that are subrounded to subangular in shape, and made up of amorphous collophane.

(2) Composite clasts that are subrounded to subangular in shape, up to 6 cm long, and display a chaotic (randomly oriented) texture (Fig. 6a). They contain a complex mixture of silt to medium-grained sand-sized allochems, composed of quartz, feldspar, mica flakes, pyrite and other opaques, rip-up shale clasts, glauconite peloids, other heterogeneous phosphatic intraclasts and bioclasts. The latter are largely composed of trilobite sclerites, brachiopod valves, hexactinellid sponge spicules and chancelloriid sclerites (Fig. 6b). Thin-sections reveal that the phosphatization involved occlusion of intra- and interparticle porosity, rim cement overgrowth, and partial replacement of interparticle micrite by fluorapatite and collophane.

(3) Clasts bearing phosphatized microbial pseudomorphs. Two kinds of microbial populations are distinguished: (1) microbial biofilms or microstromatolites that grew on inter-particle pores produced complex phosphatic crusts and anisotropic phosphatic coatings (Fig. 6c, d) and (2) dispersed void-filling botryoidal (globular clusters) textures similar to ovoidal to rod-like microbial colonies (up to 5 μm in diameter). The excellent textural preservation shows that the concentration and precipitation of phosphate occurred prior to and independently from the decay of the microbial organic matter, during a very early stage of diagenesis.

Homogeneous clasts were sourced from centimetre-thick hardground crusts or nodules, whereas the polymictic and polyphasic character of the heterogeneous clasts indicates that discrete phosphogenic episodes alternated with reworking and depositional events. Coeval reworking of pyrite (formed under reducing and sulphidic conditions below the seafloor/water interface) is shown by mechanical breakage and the polyphase nature of some composite pyrite agglomerates, and that of heterogeneous clasts by growth of gradually thickened fluorapatite coatings or rims around single or aggregated bioclasts and lithoclasts.

Two processes must be distinguished: phosphogenesis and phosphate concentration. Phosphogenesis is a biogeochemical process governed by microbially mediated Eh and pH of bottom and pore waters, dissolved chemical elements and sedimentary rates, whereas the concentration of the authigenic minerals is related

https://doi.org/10.1017/S0016756809990021 Published online by Cambridge University Press

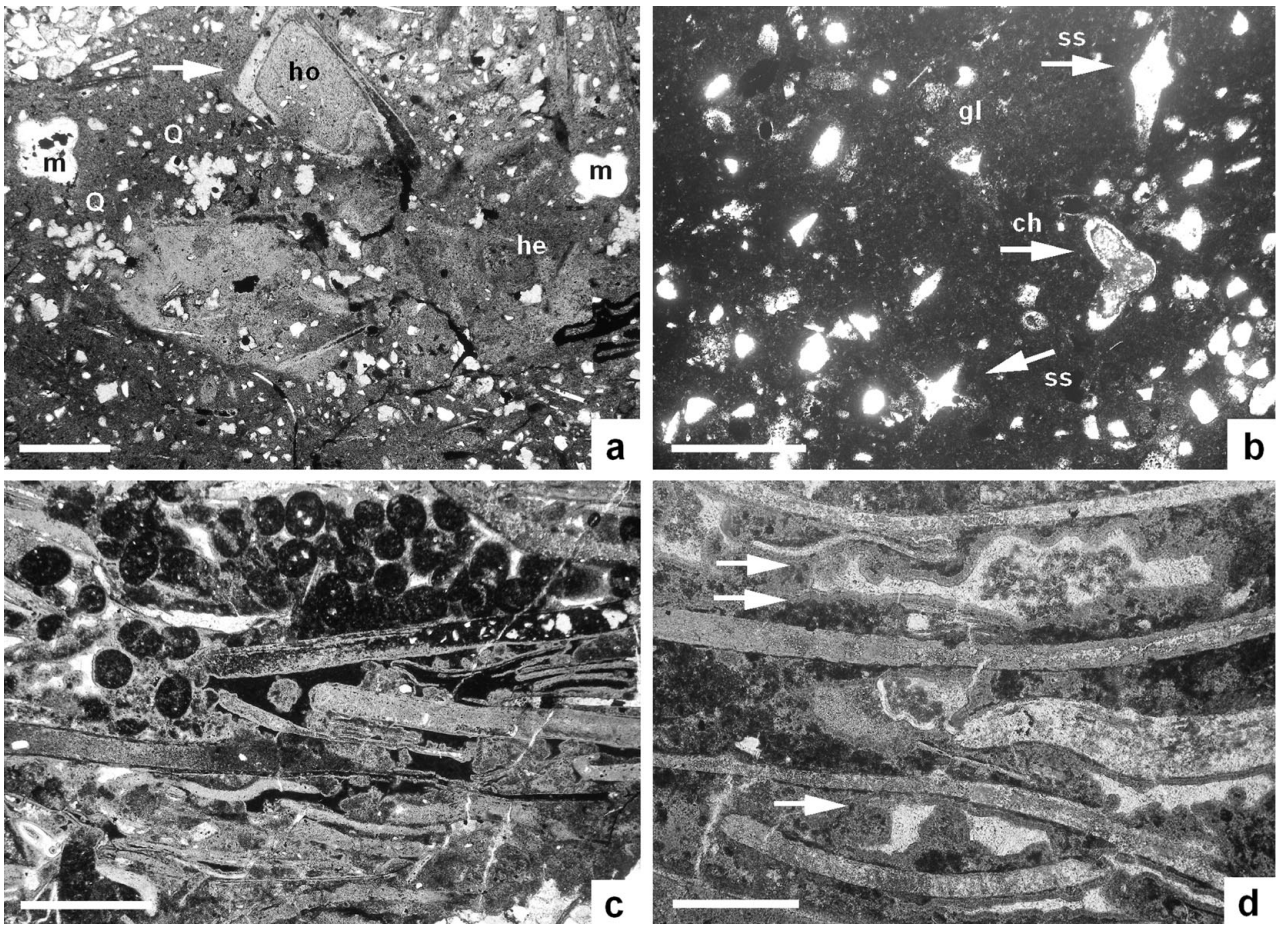

Figure 6. Thin-section photomicrographs of phosphoritic clasts. (a) Polyphase clast bearing homogeneous clasts (ho) encrusted by apatitic lamellae, heterogeneous clasts (he), engulfed quartz (Q), four-lobed mosaics of micro- and cryptocrystalline silica (similar to volcanic glass shards; m), and glauconite; level B of the Gislöv Formation at Forsemölla; scale bar = 1 mm. (b) Detail of a heterogeneous phosphoritic clast including sections of chancelloriids (ch) and hexactinellid sponge spicules (ss), quartz and glauconite (gl) clasts; level E of the Gislöv Formation at Brantevik; scale bar = 500 μm. (c) Bioclastic–peloidal packstone partly replaced into apatite: original peloids and bioclasts are wholly replaced by apatite, whereas the remaining voids were occluded by apatite, calcite and pyrite; level B of the Gislöv Formation at Forsemölla; scale bar = 2 mm. (d) Detail of cements occluding primary pores, composed of microbial crusts of apatite (displaying both microstromatolitic and globular textures), and mosaics of calcite; level B of the Gislöv Formation at Forsemölla; scale bar = 2 mm.

to hydraulic reworking and/or winnowing processes (Krajewski *et al*. 1994; Föllmi, 1996; Sagemann *et al*. 1999; Briggs, 2003). In fact, the succession of repeated cycles of sedimentation, phosphate concentration and reworking led to multi-event phosphate deposits rich in heterogeneous clasts. We concur with Notholt & Brasier (1986) that the major source of phosphorus in the Cambrian of Scania is associated with upwelling waters. According to palaeomagnetic reconstructions, upwelling was probably induced by the northeast trade winds that influenced the northwest corner of Baltica, located at a palaeolatitude of around 35° S (Torsvik & Rehnström, 2001; Cocks & Torsvik, 2005). Intense coastal upwelling might have provided a supply of nutrients to surface waters, resulting in high primary productivity followed by high organic carbon fluxes to the sea-floor, although phosphogenetic processes associated with condensation during successive drowning events cannot be ruled out (A. T. Nielsen, Copenhagen, pers. comm. 2009). The precipitation of apatite within these settings is stimulated by the production of pore-water phosphate generated through the microbial degradation of organic matter (preserved as phosphatized microbial pseudomorphs) and, in our case study, coincides with the sudden abundance of linguliformean brachiopods. The episodic character of phosphate precipitation is possible by maintaining the phosphatized particles at or near the sediment–water interface through repeated cycles of sudden burial and subsequent removal (the so-called 'Baturin cycles': Föllmi, 1996). As a result, the Scanian strata are characterized by current-dominated sedimentary regimes with correspondingly low net sedimentary accumulation rates.

Several key requirements are needed for phosphate precipitation: (1) an excess supply of P_2O_5, commonly related to biogenic sources, (2) a limited or depleted supply of Mg, (3) suitable high pH conditions and (4) a slow rate of deposition of clastic or ferruginous sediments (Marshall-Neill & Ruffell,

https://doi.org/10.1017/S0016756809990021 Published online by Cambridge University Press

2004). Phosphate clasts and nodules observed in the Gislöv and Forsemölla units often encapsulate glauconitic remains, implying early glauconite formation. As Mg is required for glauconitization, glauconite precipitation necessarily depleted the pore water content of Mg, favouring precipitation of phosphate. The coeval occurrence of phosphate and glauconite debris coexisting in polyphase clasts suggests that they either precipitated simultaneously or during alternating phases with no compaction or diagenetic alteration in between. Glauconitization indicates enrichment of iron in sediment pore waters, subsequently precipitated as pyrite. An early-diagenetic suboxic environment provided the right conditions for phosphogenesis, glauconitization and the coeval presence of authigenic and reworked pyrite. This contrasts with the burrowing and the rich and diverse benthic fauna, reflecting syndepositional well-oxygenated conditions.

7. C- and O-isotope stratigraphy

Stable carbon and oxygen isotope analyses were performed on bulk rock samples from fresh intervals of the Gislöv Formation and the Forsemölla and Exsulans limestone beds at Brantevik, a section well constrained biostratigraphically (Bergström & Ahlberg, 1981). Rock samples were selected in micritic-to-microsparitic matrix with sparse skeletal content, where neither intraparticular nor shelter cements are visible. Clean matrix was drilled with a dental microdrill and the powdered samples were digested in 100 % phosphoric acid at 25 °C. The resulting CO_2 gas was analysed using an ISOPRIME mass-spectrometer for isotopic analysis at the University of Salamanca (for details, see Al-Assam, Taylor & South, 1990). The isotopic composition of calcite is expressed by the conventional δ notation relative to the V-PDB reference (Craig, 1957); $\delta = [(Rs/Rr) - 1] * 1000$, where $R = {}^{18}O/{}^{16}O$ or ${}^{13}C/{}^{12}C$, respectively, in the sample and in the reference. Analytical reproducibility (1σ) is 0.1 ‰ for $\delta^{18}O$ and $\delta^{13}C_{carb}$.

We analysed 12 samples for carbonate $\delta^{13}C$ and $\delta^{18}O$, spanning a mixed stratigraphic interval of 1.65 m, in which the hardground and phosphatized tops of each limestone bed were not sampled, in order to avoid influence of organic-rich substrates (Fig. 7). The $\delta^{13}C_{carb}$ background values for the section gradually decrease from −1.4 to −7.9 ‰ through the Gislöv–Forsemölla units. After the generalized drowning of the Scanian platform, associated with widespread deposition of kerogenous shales, the recovery of carbonate productivity (Exsulans Limestone Bed) displays a sharp increase of $\delta^{13}C_{carb}$ over 15 cm, reaching a positive value of +0.89 ‰.

The diagenetic processes capable of causing changes in the oxygen- and carbon-isotope composition of marine carbonate components include neomorphism and recrystallization, re-equilibration with fluids of different isotope composition, and precipitation of

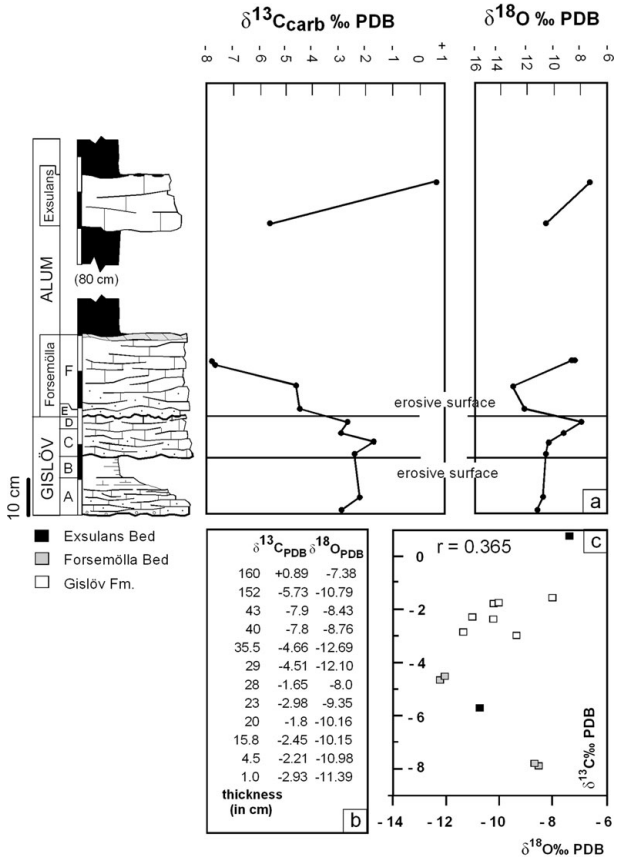

Figure 7. (a) Stratigraphic log of the Brantevik section with chemostratigraphic data. (b) $\delta^{13}C_{carb}$ and $\delta^{18}O$ values. (c) $\delta^{13}C_{carb}$ ‰v. $\delta^{18}O$ ‰cross-plot; r = coefficient of correlation.

isotopically different diagenetic carbonate phases (e.g. Glumac & Walker, 1998). Fluctuation of $\delta^{18}O$ values in the studied limestones ranges from −7.38 to −12.69 ‰. These values fit well with similar analyses compiled from Cambrian tropical low-Mg calcite-walled brachiopods (probably yielding the closer proxy to real sea-water chemistry), which vary from −7 to −12 ‰ (Wadleigh & Veizer, 1992; Veizer *et al*. 1999). In addition, the studied limestones were not significantly exposed either to meteoric waters or to marine-meteoric waters of the mixing zone, because of the wide variability of $\delta^{18}O$ values, and lack of covariance between $\delta^{13}C$ and $\delta^{18}O$ values (see coefficient of correlation, r = 0.36), respectively (Brand & Veizer, 1980; Allen & Matthews, 1982). Although a relative depletion of $\delta^{18}O$ values, reflecting a diagenetic resetting and post-depositional alteration, cannot be rejected, we consider that the $\delta^{13}C$ values were negligibly altered.

As a result, the $\delta^{13}C$ composite curve (formed by segments separated by erosive discontinuities) of the lower–middle Cambrian transition in Scania is strongly asymmetric, attaining minimum values (shift to −7.9 ‰) close to the top of the earliest middle Cambrian Forsemölla Limestone Bed. Higher up, after a demise in carbonate productivity and deposition of kerogenous shales related to drowning, the Exsulans

https://doi.org/10.1017/S0016756809990021 Published online by Cambridge University Press

Limestone Bed records a pronounced rise in $\delta^{13}C$ to enriched values (+0.89 ‰), followed again by a new demise of carbonate productivity. The initial negative shift from low to moderately negative values coincides with the onset of the three deepening-upward parasequences described above, whereas the subsequent positive trend coincides with sedimentary features that suggest flooding and drowning in an open-marine setting.

8. Chemostratigraphic comparison with other palaeocontinental margins

Similar asymmetric fluctuations of $\delta^{13}C$ across the lower–middle Cambrian transition are known from other basins, although intercontinental correlation within the lower–middle Cambrian transitional interval is hampered by the strongly provincial character of the faunas. In the Siberian Platform, a negative $\delta^{13}C$ shift to nearly −2 ‰ occurs close to the Botoman–Toyonian boundary, post-dating a turnover of shallow-platform trilobites, and followed by a rapid decline in archaeocyathan diversity (Debrenne, 1991; Zhuravlev, 1998). Brasier *et al.* (1994) reported that the subsequent Toyonian–early middle Cambrian interval was characterized by a gradual increase in $\delta^{13}C$ values. This was also documented by Brasier & Sukhov (1998) in the middle Botoman–late Amgan Kuonamka Formation, dominated by organic-rich argillaceous carbonates deposited under starved-basin conditions, where $\delta^{13}C$ values gradually turned from mainly negative values to positive at the top of the Toyonian. This corresponds with a $\delta^{13}C$ curve recorded from coeval Ordian to early Templetonian carbonates from the Georgina Basin (Donnelly, Shergold & Southgate, 1988; Shergold, 1995), and a similar gradual increase in $\delta^{13}C$ values punctuated by positive shifts across the lower–middle Cambrian transition in the western Mediterranean region (West Gondwana; Wotte *et al.* 2007).

Another distinct negative shift in $\delta^{13}C$ has been documented from the Laurentian lower–middle Cambrian boundary interval in the Great Basin (Montañez *et al.* 2000), where the succession is relatively conformable and complete. In Laurentia, the onset of a large negative excursion ($\geq$ 4 ‰ to negative $\delta^{13}C$ values) is located just beneath an extinction level at the lower–middle Cambrian boundary (Palmer, 1998*a*, *b*). This negative carbon isotope excursion is interpreted as recording: (1) the introduction of ^{13}C-depleted anoxic waters onto shallow-water carbonate platforms during the latest early Cambrian, (2) a decrease in organic carbon burial due to major biomass reduction or (3) a major decrease in primary producers and global oceanic productivity (Saltzman *et al.* 2000; Álvaro *et al.* 2008). The hypothesis that an anoxic water column developed below the mixed surface layer, at least locally, during the latest early Cambrian and before a major transgression, has recently received further support from sulphur isotope data (Hough *et al.* 2006). Sea-water $\delta^{13}C$ values from the upper part of the middle Cambrian in the Great Basin exhibit high-frequency fluctuations (shifts of a magnitude as high as 4 ‰) around a base-line value of −0.5 ‰, but the curve shows a broadly progressive fall in values during the early middle Cambrian.

No distinct shift in the carbon-isotopic composition was recognized by Guo *et al.* (2005) at the lower–middle Cambrian transition in the Guizhou Province of South China, where there is a decreasing trend in $\delta^{13}C$ values from positive values in the upper lower Cambrian to negative values in the lower part of the middle Cambrian. In contrast, the corresponding interval in the Wangcun section, Hunan, South China, is characterized by a distinct negative shift of about 4 ‰ in $\delta^{13}C$ values across the Qiangdongian–Wulingian transition (Zhu *et al.* 2004). These authors have also described two similar excursions across the lower–middle Cambrian transitional interval in the Jiagou and Bagongshan sections of the Anhui Province, North China, although biostratigraphic data allowing precise correlation between these two palaeogeographically separated blocks are not yet available. Zhu *et al.* (2004) proposed a direct chronostratigraphic correlation of the Qiangdongian–Wulingian transition of South China with the Laurentian *Olenellus–Plagiura* transition, based on this negative excursion and the FAD of *Ptychagnostus atavus* in these successions. Thus, the Laurentian $\delta^{13}C$ negative shift at the *Olenellus–Plagiura* transition and the Qiangdongian–Wulingian negative $\delta^{13}C$ peak in South China (Zhu *et al.* 2004) correspond well with the Redlichiid–Olenellid Extinction Carbon isotope Excursion (ROECE) at the boundary between Series 2 and 3 of the Global standard Cambrian (Zhu, Babcock & Peng, 2006). The ROECE excursion can be tentatively identified also in Scania, albeit partly affected by the gap between the Gislöv Formation and the Forsemölla Limestone Bed.

9. Subtropical versus temperate waters

Throughout late Neoproterozoic and Cambrian times, Baltica lay at southerly latitudes ($\sim$ 30–60° S: Cocks & Torsvik, 2005) and was geographically inverted: present-day southern Baltica faced the equator and NW Baltica the NW Gondwanan margin. A key palaeomagnetic datum from late Cambrian Alum Shales sampled in the Forsemölla–Andrarum area places Scania at around 35° S (Torsvik & Rehnström, 2001). Are these palaeomagnetic data supported by the aforementioned facies associations?

The four episodes of shell-dominated carbonate productivity, represented by the onset of the Gislöv, Forsemölla and Exsulans units, developed on an unrimmed platform bordering NW Baltica. Among other primary factors, they were directly controlled by terrigenous input, carbonate productivity, accommodation space and nutrient supply. Frame-building fabrics

https://doi.org/10.1017/S0016756809990021 Published online by Cambridge University Press

are absent, and dominant carbonate facies are grainy (or shelly), and were hydrodynamically controlled by the action of traction currents. Biostratinomic processes were dominated by post-mortem skeletal disarticulation and fragmentation, and carbonate mud was commonly winnowed off-platform. The carbonate mud appears to be homogeneous, sometimes mottled as a consequence of burrowing, but rarely pelleted, except within phosphatized clasts, in which spherical aggregates of micrite (up to 50 μm in diameter) are common (Fig. 6c). Microbial activity was pervasive, as indicated by the widespread development of microboring and phosphatized microbes, but did not develop centimetre-scale stromatolites or thrombolites.

The carbonate sea-floor supported a prolific epibenthic biota, which produced abundant skeletal debris, and a significant endobenthic biota, as suggested by the presence of macroburrowing. The greatest production of skeletal grains was associated with the proliferation of multi-element organisms (such as chancelloriids, echinoderms, sponges, trilobites and brachiopods) that rapidly disintegrated after death into their constituent parts, showing abundant signs of mechanical breakage, abrasion and considerable rounding. The benthic communities were dominated by fixed, mainly filter-feeding nonreefal chancelloriid–echinoderm–sponge meadows (the CES community *sensu* Álvaro & Vennin, 1997). The coarsest fraction of the skeletons was transported short distances (e.g. Exsulans Limestone Bed), while the smallest grains were redistributed by currents across the platform resulting in episodic low-angle sheets or shoals of loose hydrodynamic skeletal sediment that covered the open sea-floor, intensely affected by current and storm washing and winnowing (e.g. Gislöv Formation and Forsemölla Limestone Bed).

The hydrodynamic regime is reflected by the episodic presence of intra-bed erosive surfaces, overlain by grading structures, and not encrusted by microbial veneers or mats. The absence of these microbial crusts is a key difference between the Gislöv and Forsemölla units and another coeval and mixed, condensed succession, namely, the Brèche à *Micmacca* in the Atlas Mountains, Morocco (Álvaro & Clausen, 2006, 2008; Álvaro *et al.* 2007). The limestone interbeds of the latter also display the episodic development of chancelloriid–echinoderm–sponge meadows, affected by intensive bottom current abrasion and winnowing (responsible for the onset of intra-bed erosive diastems), and an abundance of volcanogenic, phosphate and glauconite clasts. However, in Morocco, the aforementioned diastems were encrusted with microbial mats. The main hydrodynamic factors that controlled biomat development were: low sediment accumulation rates, early lithification (grainstone facies is common), and substrate stability (the microtopography of the shelly/grainy sea-floor provided growth space, where the cemented shell surface was permanently suitable for microbial nucleation). Both the limestones of the Brèche à *Micmacca* and those of Scania are composite event-concentration, low-relief shoal complexes composed of parautochthonous bioclastic assemblages. These units can be described as 'hiatal accumulations' (*sensu* Kidwell & Bosence, 1991) because of the subdivision of the coquinas by minor discontinuities and the composite, multiple-event nature of the shell concentrations.

Under what conditions do microbial crusts form during depositional hiatuses? Based on field and laboratory studies, under normal oxygenated conditions and in the absence of grazers, brief hiatuses can favour development of microbial laminated crusts, whereas prolonged episodes or longer hiatuses can be characterized by microboring infestation (e.g. Reid *et al*. 2003). As a result, there is a limit to the time span related to these hiatal processes, as longer hiatal episodes can result in development of eukaryotic algal communities, which do not form laminated structures. Therefore, the absence of microbial mats in the lower–middle Cambrian boundary interval of Scania cannot be directly considered as an argument to support temperate waters.

Nutrient supply is another key factor to understand proliferation of microendoliths (Peterhänsel & Pratt, 2001), poorly developed in the Brèche à *Micmacca*. It can result from terrestrial influx of organic matter, marine transgression, or upwelling. Eutrophic conditions are characterized by high and oscillating levels of nutrient supply, and high net productivity, which contrast with the low and stable nutrient supply and lower net productivity of oligotrophic conditions. As a result, levels of bioerosion are high in eutrophic areas (characterized, for instance, by microendolithic infestation), associated with low or irregular patterns of carbonate productivity, and relatively low in oligotrophic environments (Wood, 1993; Brasier, 1995). Glauconite formation and phosphogenesis may also indicate the presence of increased levels of K and P, two nutritive elements. Therefore, all evidence indicates coastal upwelling on the NW corner of Baltica as a direct cause of enhanced nutrient mobilization, analogous to modern subtropical unrimmed platforms (Vogel *et al.* 2000).

Another palaeogeographic area, where the lower–middle Cambrian transition is recognized as an erosive unconformity covered by limestones and limestone/black shale alternations, is the Georgina Basin, Australia. In the Hay River–Mount Whelan region, Donnelly, Shergold & Southgate (1988) reported the series boundary at the contact of the Red Heart Dolostone and Lower Hay River formations. The lower part of the latter formation consists of phosphatic mudstone and wackestone that alternate with centimetre-thick, phosphatic hardgrounds. The palaeoenvironment subsequently recorded the alternation of winnowed (well-oxygenated) and calm (anoxic) substrates, mimicking the stratigraphy of the lower part of the Alum Shales. However, the Australian sea-floor neither recorded permanent reworking nor pervasive episodic erosion, allowing for the preservation of intact phosphatic hardgrounds, which are absent in Scania.

https://doi.org/10.1017/S0016756809990021 Published online by Cambridge University Press

10. Conclusions

This paper offers a high-resolution stratigraphic analysis of the unconformity-bearing mixed strata through the lower–middle Cambrian boundary interval in Scania, southern Sweden. The transition is characterized by a distinct shift in the style of sedimentation, changing from siliciclastics to carbonates and then kerogenous shales. Deposition was associated with the formation of numerous erosive unconformities. The transgression led to a cratonward shift of the depocentre in the NW corner of Baltica, leaving Scania in an offshore, sediment-starved position.

The lower–middle Cambrian boundary interval in Scania is characterized by three condensed shell limestone beds, with a total thickness of up to 1.2 m, and lithostratigraphically grouped in the Gislöv Formation and the Forsemölla and Exsulans Limestone beds (Alum Shale Formation). The strata display a combination of skeletal carbonate productivity, episodic precipitation of phosphate hardgrounds and nodules (some of them microbially mediated), glauconite precipitation, widespread microboring and polyphase reworking on a platform bordering the NW corner of Baltica. The shell accumulations of the Gislöv and Forsemölla limestone units can be subdivided into three deepening-upward, wave- and storm-dominated parasequences, separated by distinct erosive unconformities. Biostratigraphically, the parasequences correspond to the *Holmia kjerulfi*, *Ornamentaspis*? *linnarssoni* and *Ptychagnostus gibbus* zones, the latter two generally being separated by a stratigraphic gap that includes the middle Cambrian *Acadoparadoxides oelandicus* Superzone.

A prolific epibenthic biota, dominated by filter-feeding nonreefal chancelloriid–echinoderm–sponge meadows (the so-called CES community), rich in dwelling trilobites and brachiopods, was subjected to high-energy conditions. The absence of microbial mats or veneers encrusting the erosive surfaces of these event-concentration low-relief shoal complexes may be related to longer hiatal episodes resulting in microboring infestation. The limestones do not indicate a starvation of terrigenous supply, but rather a decrease (some beds are true calcarenites) and a subtropical palaeoclimate suitable for substantial episodes of carbonate productivity capable of avoiding terrigenous poisoning.

Three kinds of apatite debris are recognized: homogeneous, composite and microbial pseudomorph-bearing clasts. The major source of phosphorus is probably associated with upwelling waters, probably induced by the northeast trade winds that influenced the NW corner of Baltica, located at a palaeolatitude of around 35° S. An abundance of nutrients resulted in intervals with high primary productivity, eutrophic conditions, glauconite formation (which depleted the pore water content of Mg, favouring phosphogenesis, in some case microbially mediated) and microendolithic infestation. Analogous to the nutrient response in modern tropical carbonate environments, the impact of bioerosion in the shell substrates is likely linked to excess nutrient flux. An early-diagenetic mildly reducing environment is suggested by the presence of authigenic (subsequently reworked) pyrite, which contrasts with the syndepositional normal oxygenated conditions reflected by the abundance of benthic macrofossils and macroburrowing.

The overlying kerogenous shales (Alum Shale) represent the onset of a general drowning episode throughout Baltica, and mark a turning point in the style of sedimentation. The rise in relative sea-level may have been important in the establishment of biogeographic connections between the middle Cambrian Acado-Baltic Province, and in the exchange of nutrient-enriched waters.

C- and O- isotope stratigraphy across the lower–middle Cambrian boundary interval allows recognition of an asymmetric $\delta^{13}C$ composite curve attaining minimum values (negative shift to −7.9 ‰) close to the top of the earliest middle Cambrian Forsemölla Limestone Bed, subsequently followed by a pronounced rise in $\delta^{13}C$ to enriched values (+0.89 ‰) in the Exsulans Limestone Bed, and finally succeeded by a generalized drowning, linked to a dramatic demise of carbonate productivity. Although considerably affected by the gaps included in these Scanian unconformity-bearing mixed strata, the negative chemostratigraphic shift fits well with other excursions recorded across the *Olenellus–Plagiura* and the Qiangdongian–Wulingian transitions (in Laurentia and South China, respectively), and may represent the global ROECE signal.

Acknowledgements. We thank D. Kaljo (Tallinn) and L. E. Popov (Cardiff) for stratigraphic and bibliographic information, K. Föllmi (Neuchâtel) for helpful comments on a previous version of the manuscript, and G. E. Budd (Uppsala), A. T. Nielsen (Copenhagen), and an anonymous referee for useful and constructive criticism. This paper is a contribution to the *lower–middle Cambrian boundary Working Group* of the *International Subcommission on Cambrian Stratigraphy*, Spanish project CGL 2006–13533 from the Ministerio de Ciencia and FEDER, and French project ANR JC07_194555 from CNRS-USAR. PA is indebted to the Swedish Research Council (VR) and the Crafoord Foundation for their financial support.

References

AHLBERG, P. 1983. A Lower Cambrian trilobite fauna from Jämtland, central Scandinavian Caledonides. *Geologiska Föreningens i Stockholm Förhandlingar* **105**, 349–61.

AHLBERG, P. 1998. Cambrian shelly faunas and biostratigraphy of Scandinavia. In *Guide to excursions in Scania and Västergötland, Southern Sweden* (ed. P. Ahlberg), pp. 5–9. *Lund Publications in Geology* **141**.

AHLBERG, P. & BERGSTRÖM, J. 1978. Lower Cambrian ptychopariid trilobites from Scandinavia. *Sveriges Geologiska Undersökning Ca* **49**, 1–41.

AHLBERG, P. & BERGSTRÖM, J. 1998. The Cambrian of Scania. In *Guide to excursions in Scania and Västergötland, Southern Sweden* (ed. P. Ahlberg), pp. 20–3. *Lund Publications in Geology* **141**.

https://doi.org/10.1017/S0016756809990021 Published online by Cambridge University Press

AL-ASSAM, I., TAYLOR, B. E. & SOUTH, B. 1990. Stable isotope analysis of multiple carbonate samples using selective acid extraction. *Chemical Geology* **80**, 119–25.

ALLEN, J. R. & MATTHEWS, R. K. 1982. Isotopic signature associated with early meteoric diagenesis. *Sedimentology* **29**, 791–817.

ÁLVARO, J. J. & CLAUSEN, S. 2005. Major geodynamic and sedimentary constraints on the chronostratigraphic correlation of the Lower–Middle Cambrian transition in the western Mediterranean region. *Geosciences Journal* **9**, 145–60.

ÁLVARO, J. J. & CLAUSEN, S. 2006. Microbial crusts as indicators of stratigraphic diastems in the Cambrian *Micmacca* Breccia, Moroccan Atlas. *Sedimentary Geology* **185**, 255–65.

ÁLVARO, J. J. & CLAUSEN, S. 2008. Paleoenvironmental significance of hiatal shelled accumulations in a Cambrian intracratonic aborted rift, Atlas Mountains, Morocco. In *Dynamics of Epeiric Seas* (eds B. R. Pratt & C. Holmden), pp. 39–54. Geological Association of Canada, Special Paper no. 48.

ÁLVARO, J. J. & VENNIN, E. 1997. Episodic development of Cambrian eocrinoid–sponge meadows in the Iberian Chains (NE Spain). *Facies* **37**, 49–64.

ÁLVARO, J. J. & VENNIN, E. 1998. Stratigraphic signature of a terminal Early Cambrian regressive event in the Iberian Peninsula. *Canadian Journal of Earth Sciences* **35**, 402–11.

ÁLVARO, J. J., ELICKI, O., GEYER, G., RUSHTON, A. W. A. & SHERGOLD, J. H. 2003. Palaeogeographical controls on the Cambrian trilobite immigration and evolutionary patterns reported in the western Gondwana margin. *Palaeogeography, Palaeoclimatology, Palaeoecology* **195**, 5–35.

ÁLVARO, J. J., ARETZ, M., BOULVAIN, F., MUNNECKE, A., VACHARD, D. & VENNIN, E. 2007. Fabric transitions from shell accumulations to reefs: an introduction with Palaeozoic examples. In *Palaeozoic Reefs and Bioaccumulations: Climatic and Evolutionary Controls* (eds J. J. Álvaro, M. Aretz, F. Boulvain, A. Munnecke, D. Vachard & E. Vennin), pp. 1–16. Geological Society of London, Special Publication no. 275.

ÁLVARO, J. J., BAULUZ, B., SUBÍAS, I., PIERRE, C. & VIZCAÏNO, D. 2008. Carbon chemostratigraphy of the Cambrian–Ordovician transition in a midlatitude mixed platform, Montagne Noire, France. *Geological Society of America Bulletin* **120**, 962–75.

AXHEIMER, N. & AHLBERG, P. 2003. A core drilling through Cambrian strata at Almbacken, Scania, S. Sweden: trilobites and stratigraphical assessment. *GFF* **125**, 139–56.

AXHEIMER, N., AHLBERG, P. & CEDERSTRÖM, P. 2007. A new lower Cambrian eodiscoid trilobite fauna from Swedish Lapland and its implications for intercontinental correlation. *Geological Magazine* **144**, 953–61.

BABCOCK, L. E., PENG, S. C., GEYER, G. & SHERGOLD, J. H. 2005. Changing perspectives on Cambrian chronostratigraphy and progress toward subdivision of the Cambrian System. *Geosciences Journal* **9**, 101–6.

BENGTSON, S. 1976. The structure of some Middle Cambrian conodonts, and the early evolution of conodont structure and function. *Lethaia* **9**, 185–206.

BERGSTRÖM, J. & AHLBERG, P. 1981. Uppermost Lower Cambrian biostratigraphy in Scania, Sweden. *Geologiska Föreningens i Stockholm Förhandlingar* **103**, 193–214.

BERGSTRÖM, J. & GEE, D. G. 1985. The Cambrian in Scandinavia. In *The Caledonide Orogen – Scandinavia and Related Areas* (eds D. G. Gee & B. A. Sturt), pp. 247–71. London: John Wiley and Sons.

BRAND, U. & VEIZER, J. 1980. Chemical diagenesis of multicomponent carbonate system. 1. Trace elements. *Journal of Sedimentary Petrology* **50**, 1219–50.

BRASIER, M. D. 1995. Fossil indicators of nutrient levels. 1. Eutrophization and climatic change. In *Marine Palaeoenvironmental Analysis from Fossils* (eds D. W. J. Bosence & P. A. Allison), pp. 113–32. Geological Society of London, Special Publication no. 83.

BRASIER, M. D. & SUKHOV, S. S. 1998. The falling amplitude of carbon isotope oscillations through the Lower to Middle Cambrian: Northern Siberia data. *Canadian Journal of Earth Sciences* **35**, 353–73.

BRASIER, M. D., CORFIELD, R. M., DERRY, L. A., ROZANOV, A. YU. & ZHURAVLEV, A. YU. 1994. Multiple $\delta^{13}C$ excursions spanning the Cambrian explosion to the Botoman crisis in Siberia. *Geology* **22**, 455–8.

BRIGGS, D. E. G. 2003. The role of decay and mineralization in the preservation of soft-bodied fossils. *Annual Review of Earth and Planetary Sciences* **31**, 275–301.

BROMLEY, R. G. 2004. A stratigraphy of marine bioerosion. In *The Application of Ichnology to Palaeoenvironmental and Stratigraphic Analysis* (ed. D. McIlroy), pp. 455–79. Geological Society of London, Special Publication no. 228.

BROMLEY, R. G. & ASGAARD, U. 1993. Endolithic community replacement on a Pliocene rocky coast. *Ichnos* **2**, 93–116.

BRØGGER, W. C. 1886. Om alderen af Olenelluszonen i Nordamerika. *Geologiska Föreningens i Stockholm Förhandlingar* **8**, 182–213.

CATUNEAU, O., ABREU, V., BHATTACHARYA, J. P., BLUM, M. D., DALRYMPE, R. W., ERIKSSON, P. G., FIELDING, C. R., FISHER, W. L., GALLOWAY, W. E., GIBLING, M. R., GILES, K. A., HOLBROOK, J. M., JORDAN, R., KENDALL, C. G. ST. C., MACURDA, B., MARTINSEN, O. J., MIALL, A. D., NEAL, J. E., NUMMEDAL, D., POMAR, L., POSAMENTIER, H. W., PRATT, B. R., SARG, J. F., SHANLEY, K. W., STEEL, R. J., STRASSER, A., TUCKER, M. E. & WINKER, C. 2009. Towards the standardization of sequence stratigraphy. *Earth-Science Reviews* **92**, 1–33.

CHAZOTTE, V., Le CHAMPION-ALSUMARD, T. & PEYROT-CLAUSADE, M. 1995. Bioerosion rates on coral reefs: interactions between macroborers, microborers and grazers (Moorea, French Polynesia). *Palaeogeography, Palaeoclimatology, Palaeoecology* **113**, 189–98.

COCKS, L. R. M. & TORSVIK, T. H. 2005. Baltica from the late Precambrian to mid-Palaeozoic times: the gain and loss of a terrane's identity. *Earth-Science Reviews* **72**, 39–66.

CRAIG, H. 1957. Isotopic standards for carbon and oxygen and correction factors for mass spectrometric analyses of carbon dioxide. *Geochimica et Cosmochimica Acta* **12**, 133–49.

DEBRENNE, F. 1991. Extinction of the Archaeocyatha. *Historical Biology* **5**, 95–106.

DIES ÁLVAREZ, M. E., GOZALO, R., CEDERSTRÖM, P. & AHLBERG, P. 2008. Bradoriid arthropods from the lower–middle Cambrian of Scania, Sweden. *Acta Palaeontologica Polonica* **53**, 647–56.

DONNELLY, T. H., SHERGOLD, J. H. & SOUTHGATE, P. N. 1988. Anomalous geochemical signals from phosphatic Middle Cambrian rocks in the southern Georgina Basin, Australia. *Sedimentology* **35**, 549–70.

ERIKSSON, M. J. 2004. Formation and significance of a middle Silurian ravinement surface on Gotland, Sweden. *Sedimentary Geology* **170**, 163–75.

FÖLLMI, K. B. 1996. The phosphorus cycle, phosphogenesis and marine phosphate-rich deposits. *Earth-Science Reviews* **40**, 55–124.

GEE, D. G., KUMPULAINEN, R. & THELANDER, T. 1978. The Tåsjön décollement, central Swedish Caledonides. *Sveriges Geologiska Undersökning* **C742**, 1–35.

GEYER, G. 2005. The base of a revised Middle Cambrian: are suitable concepts for a series boundary in reach? *Geosciences Journal* **9**, 81–99.

GLAUB, I., GOLUBIC, S., GEKTIDIS, M., RADTKE, G. & VOGEL, K. 2007. Microborings and microbial endoliths: geological implications. In *Trace Fossils: Concepts, Problems, Prospects* (ed. W. Miller III), pp. 368–81. Amsterdam: Elsevier.

GLAUB, I. & VOGEL, K. 2004. The stratigraphic record of microborings. *Fossils and Strata* **51**, 126–35.

GLUMAC, B. & WALKER, K. R. 1998. A Late Cambrian positive carbon-isotope excursion in the southern Appalachians: relation to biostratigraphy, sequence stratigraphy, environments of deposition, and diagenesis. *Journal of Sedimentary Research* **68**, 1212–22.

GREILING, R. O., JENSEN, S. & SMITH, A. G. 1999. Vendian–Cambrian subsidence of the passive margin of western Baltica – application of new stratigraphic data from the Scandinavian Caledonian margin. *Norsk Geologisk Tidsskrift* **79**, 133–44.

GUO, QING-JUN, STRAUSS, H., LIU, CONG-QIANG, ZHAO, YUAN-LONG, PI, DAO-HUI, FU, PING-QING, ZHU, LI-JUN & YANG, RUI-DONG. 2005. Carbon and oxygen isotopic composition of Lower to Middle Cambrian sediments at Taijiang, Guizhou Province, China. *Geological Magazine* **142**, 723–33.

HOUGH, M. L., SHIELDS, G. A., EVINS, L. Z., STRAUSS, H. & MACKENZIE, S. 2006. A major sulphur isotope event at *c*. 510 Ma: a possible anoxic-extinction-volcanism connection during the Early–Middle Cambrian transition? *Terra Nova* **18**, 257–63.

KIÆR, J. 1917. The Lower Cambrian *Holmia* Fauna at Tømten in Norway. *Norske Videnskapsselskapets Skrifter, 1. Matematisk-Naturvidenskablig Klasse 1916* **10**, 1–140.

KIDWELL, S. M. & BOSENCE, D. W. J. 1991. Taphonomy and time-averaging of marine shelly faunas. In *Taphonomy: Releasing the Data Locked in the Fossil Record* (eds P. A. Allison & D. E. G. Briggs), pp. 115–209. Topics in Geobiology. New York: Plenum Press.

KRAJEWSKI, K. P., VAN CAPPELLEN, P., TRICHET, J., KUHN, O., LUCAS, J., MARTÍN-ALGARRA, A., PRÉVÔT, L., TEWARI, V. C., GASPAR, L., KNIGHT, R. I. & LAMBOY, M. 1994. Biological processes and apatite formation in sedimentary environments. *Eclogae Geologica Helvetiae* **87**, 701–45.

LINDSTRÖM, M. & STAUDE, H. 1971. Beitrag zur Stratigraphie der unterkambrischen Sandsteine des südlichsten Skandinaviens. *Geologica et Palaeontologica* **5**, 1–7.

MARINO, A. DE. 1980*a*. Sandstones and phosphatized calcareous sediments of the Lower Cambrian Rispebjerg Sandstone, Bornholm, Denmark. *Danmarks Geologiske Undersøgelse, II Række* **113**, 1–39.

MARINO, A. DE. 1980*b*. The upper Lower Cambrian strata south of Simrishamn Scania, Sweden: a transgressive-regressive shift through a limestone sequence. *Sveriges Geologiska Undersökning* **C 771**, 1–22.

MARSHALL-NEIL, G. & RUFFELL, A. 2004. Authigenic phosphate nodules (Late Cretaceous, northern Ireland) as condensed succession microarchives. *Cretaceous Research* **25**, 439–52.

MARTINSSON, A. 1974. The Cambrian of Norden. In *Lower Palaeozoic Rocks of the World. Volume 2. Cambrian of the British Isles, Norden, and Spitsbergen (with an Introduction to the Lower Palaeozoic Systems and an essay on the Pre-Cambrian–Cambrian Boundary)* (ed. C. H. Holland), pp. 185–283. London: John Wiley and Sons.

MOCZYDŁOWSKA, M. 1991. Acritarch biostratigraphy of the Lower Cambrian and the Precambrian-Cambrian boundary in southeastern Poland. *Fossils and Strata* **29**, 1–127.

MOCZYDŁOWSKA, M., JENSEN, S., EBBESTAD, J. O. R., BUDD, G. E. & MARTÍ-MUS, M. 2001. Biochronology of the autochthonous Lower Cambrian in the Laisvall–Storuman area, Swedish Caledonides. *Geological Magazine* **138**, 435–53.

MONTAÑEZ, I. P., OSLEGER, D. A., BANNER, J. L., MACK, L. E. & MUSGROVE, M. 2000. Evolution of the Sr and C isotope composition of Cambrian oceans. *GSA Today* **10**(5), 1–7.

NIELSEN, A. T. & SCHOVSBO, N. H. 2007. Cambrian to basal Ordovician lithostratigraphy in southern Scandinavia. *Bulletin of the Geological Society of Denmark* **53**, 47–92.

NIKOLAISEN, F. 1986. Olenellid trilobites from the uppermost Lower Cambrian Evjevik Limestone at Tømten in Ringsaker, Norway. *Norsk Geologisk Tidsskrift* **66**, 305–9.

NOTHOLT, A. J. G. & BRASIER, M. D. 1986. Proterozoic and Cambrian phosphorites – regional review. *Europe.* In *Phosphate Deposits of the World. Vol. 1. Proterozoic and Cambrian Phosphorites* (eds P. J. Cook & J. H. Shergold), pp. 91–100. Cambridge: Cambridge University Press.

PALMER, A. R. 1998*a*. A proposed nomenclature for stages and series for the Cambrian of Laurentia. *Canadian Journal of Earth Sciences* **35**, 323–8.

PALMER, A. R. 1998*b*. Terminal Early Cambrian extinction of the Olenellina: documentation from the Pioche Formation, Nevada. *Journal of Paleontology* **72**, 650–72.

PALMER, A. R. & JAMES, N. P. 1980. The Hawke Bay event: a circum-Iapetus regression near the Lower–Middle Cambrian boundary. In *The Caledonides in the U.S.A*. (ed. D. R. Wones), pp. 15–18. Department of Geological Sciences, Virginia Polytechnic Institute and State University, Memoir no. 2.

PEDERSEN, G. K. 1989. The sedimentology of Lower Palaeozoic black shales from the shallow wells Skelbro 1 and Billegrav 1, Bornholm, Denmark. *Bulletin of the Geological Society of Denmark* **37**, 151–73.

PETERHÄNSEL, A. & PRATT, B. R. 2001. Nutrient-triggered bioerosion on a giant carbonate platform masking the postextinction Famennian benthic community. *Geology* **29**, 1079–82.

REID, P., DUPRAZ, C. D., VISSCHER, P. T. & SUMNER, D. Y. 2003. Microbial processes forming marine stromatolites. In *Fossil and Recent Biofilms: a Natural History of Life on Earth* (eds W. E. Krumbein, D. M. Paterson & G. A. Zavarzin), pp. 103–18. Dordrecht: Kluwer Academic Publishers.

ROBISON, R. A., ROSOVA, A. V., ROWELL, A. J. & FLETCHER, T. P. 1977. Cambrian boundaries and divisions. *Lethaia* **10**, 257–62.

SAGEMANN, J., BALE, S. J., BRIGGS, D. E. G. & PARKES, R. J. 1999. Controls on the formation of authigenic minerals in association with decaying organic matter: An

experimental approach. *Geochimica et Cosmochimica Acta* **63**, 1083–95.

SALTZMAN, M. R., RIPPERDAN, R. L., BRASIER, M. D., LOHMANN, K. C., ROBISON, R. A., CHANG, W. T., PENG, S., ERGALIEV, E. K. & RUNNEGAR, B. 2000. A global carbon isotope excursion (SPICE) during the Late Cambrian: relation to trilobite extinctions, organic-matter burial and sea level. *Palaeogeography, Palaeoclimatology, Palaeoecology* **162**, 211–23.

SDZUY, K. 1972. Das Kambrium der acadobaltischen Faunenprovinz – Gegenwärtiger Kenntnisstand und Probleme. *Zentralblatt für Geologie und Paläontologie* **II 1972**, 1–91.

SHERGOLD, J. H. 1995. Timescales 1. Cambrian. Australian Phanerozoic timescales, biostratigraphic charts and explanatory notes (2nd series). *Australian Geological Survey Organization, Record* **1995/30**, 1–32.

STRENG, M., GEYER, G. & BUDD, G. E. 2006. A bone bed without bones: the Middle Cambrian 'fragment limestone' of Scania, Sweden. *The Palaeontological Association Newsletter* **63**, 72.

STRENG, M., HOLMER, L. E., POPOV, L. E. & BUDD, G. E. 2007. Columnar shell structures in early linguloid brachiopods – new data from the Middle Cambrian of Sweden. *Earth and Environmental Science, Transactions of the Royal Society of Edinburgh* **98**, 221–32.

TORSVIK, T. H. & REHNSTRÖM, E. F. 2001. Cambrian palaeomagnetic data from Baltica: Implications for true polar wander and Cambrian palaeogeography. *Journal of the Geological Society, London* **158**, 321–30.

VEIZER, J., ALA, D., AZMY, P., BRUCKSCHEN, P., BUHL, D., BRHUN, F., CARDEN, G. A. F., DIENER, A., EBNETH, S., GODDERIS, Y., JASPER, T., KORTE, C., PAWELLEK, F., PODLAHA, O. & STRAUSS, H. 1999. $^{87}Sr/^{86}Sr$, $\delta^{13}C$, and $\delta^{18}O$ evolution of Phanerozoic seawater. *Chemical Geology* **161**, 59–88.

VOGEL, K., GEKTIDIS, M., GOLUBIC, S., KIENNE, W. E. & RADTKE, G. 2000. Experimental studies on microbial bioerosion at Lee Stocking Island, Bahamas and One Tree Island, Great Barrier Reef, Australia: Implications for paleoecological reconstructions. *Lethaia* **33**, 190–204.

WADLEIGH, M. M. & VEIZER, J. 1992. $^{18}O/^{16}O$ and $^{13}C/^{12}C$ in lower Paleozoic brachiopods: implications for the isotopic composition of sea water. *Geochimica et Cosmochimica Acta* **56**, 431–43.

WOOD, R. 1993. Nutrients, predation and the history of reef-building. *Palaios* **8**, 526–43.

WOTTE, T., ÁLVARO, J. J., SHIELDS, G. A., BROWN, B., BRASIER, M. D. & VEIZER, J. 2007. C-, O- and Sr-isotope stratigraphy across the Lower–Middle Cambrian transition of the Cantabrian Zone (Spain) and the Montagne Noire (France), West Gondwana. *Palaeogeography, Palaeoecology, Palaeoclimatology* **256**, 47–70.

ZHU, MAO-YAN, ZHANG, JUN-MING, LI, GUO-XIANG & YANG, AI-HUA. 2004. Evolution of C isotopes in the Cambrian of China: implications for Cambrian subdivision and trilobite mass extinctions. *Geobios* **37**, 287–301.

ZHU, MAO-YAN, BABCOCK, L. E. & PENG, SHAN-CHI. 2006. Advances in Cambrian stratigraphy and paleontology: Integrating correlation techniques, paleobiology, taphonomy and paleoenvironmental reconstruction. *Palaeoworld* **15**, 217–22.

ZHURAVLEV, A. YU. 1998. Outlines of the Siberian Platform sequence stratigraphy in the Lower and lower Middle Cambrian (Lena-Aldan area). *Revista Española de Paleontología* **número extraordinario**, 105–14.

https://doi.org/10.1017/S0016756809990021 Published online by Cambridge University Press